2.1.2. DPOAEs

DPOAES were recorded and analyzed using the ILO-92 system (Otodynamics Ltd, Herts, UK). DPOAE primary tones f1 and f2 were presented at 70 dB SPL. The f2:f1 ratio was kept at 1.22, and the frequency of f2 was changed in one-third octave steps from 708 to 6299 Hz. The levels of 2f1–f2 DPOAE were recorded. DPOAE values were plotted on a DP-gram, which expresses the emission level as a function of the f2 frequency.

2.1.3. Auditory brainstem responses (ABRs)

ABRs were recorded using the Neuropack system (Nihon Kohden, Tokyo, Japan) with an electrode montage of vertex (CZ) to the ipsilateral (stimulated) ear lobe and ground to forehead (Fz). The amplifier band pass was 100–1000 Hz. Alternating-polarity click stimuli were presented monaurally at a rate of 20 Hz at 100 dB nHL. Average responses to 1024 clicks were collected in each of two experiments.

2.2. Vestibular function tests

2.2.1. Electronystagmography

The patient underwent an electronystagmography test battery consisting of spontaneous, optokinetic, positional, postural, and caloric-induced nystagmus recordings. Nystagmus was recorded using an electronystagmograph recorder (Rion, Tokyo, Japan). Caloric testing using 20 °C and ice-cold water (5 cm^3, 5 s) was used to irrigate the external auditory meatus to induce a thermal gradient across the lateral semicircular canal.

2.2.2. Vestibular evoked myogenic potentials (VEMPs)

The sternocleidomastoid (SCM) muscle was chosen as the target to record VEMPs using the Neuropack system (Nihon Kohden, Tokyo, Japan). Surface electromyographic activity was recorded from symmetrical sites over the upper half of each SCM, with a reference electrode over the sternal attachment site of the contralateral SCM. The patient was laid supine on a bed and asked to raise and orient his head contralateral to the tested ear to maximally activate the SCM ipsilateral to the stimulation. Responses to 200 short-tone bursts (105 dB nHL, 500 Hz) were recorded at 100-ms intervals over a band pass of 500–1500 Hz.

2.3. Neuroimaging studies

2.3.1. High-resolution computed tomography (HRCT)

The protocol for HRCT included scanning with a multi-slice computed tomography scanner (Sensation 64; Siemens Medical Solutions, Inc., Malvern, PA, USA). Images were acquired with direct axial sequences using a spiral scan procedure with a 1.0-mm collimation. Data were reconstructed with a slice thickness of 1.0 mm using a bone algorithm.

2.3.2. Magnetic resonance imaging (MRI)

The patient was scanned on a 1.5-T MRI machine (Signa EXITE 1.5T, General Electric, Fairfield, CT, USA) with surface and head coil. Axial three-dimensional fast imaging employing steady-state acquisition (FIESTA, repetition time, 9.3 ms/echo time, 3.3 ms; scan thickness 1.0 mm) was performed. The axial images were reconstructed in the oblique sagittal plane traversing the internal auditory canal (IAC), producing cross-sectional images that visualize the neural structures of the IAC.

2.4. Homology modeling of OPA1 and ligand fitting

The crystal structure of the GTPase domain of rat dynamin 1 (PDB ID: 2AKA) was used as a template in homology modeling because the GTPase domain of rat dynamin 1 is closely related to that of OPA1 in both function and structure (32% amino acid sequence identity). A program package for protein engineering and drug design, BIOCES[E] (NEC Corp., Tokyo, Japan) [7], was used for a series of molecular modeling. This package runs on an OCATANE2 (Silicon Graphics Inc., Fremont, CA, USA). The GTP molecule of Ras-GTP (PDB ID: 5P21) was fitted into the corresponding active site of the OPA1 model using DALI (http://ekhidna.biocenter.helsinki.fi/dali_server/) [8]. The p.R445H mutation structure was superimposed on the native structure (backbone atoms only) and displayed using UCSF Chimera (http://www.cgl.ucsf.edu/chimera/) [9].

3. Case report

The patient is a 28-year-old man who first presented with sudden optic atrophy at the age of 17 years. Clinical history of vision disorder and the result of genetic test have been reported [10]. In brief, he received a detailed examination for visual function at age 21. His best corrected visual acuity was 20/200 in both eyes. He had atrophy of the optic disks, central scotoma, and generalized bilateral dyschromatopsia. As a result, the patient was diagnosed with ADOA, and a genetic examination revealed a heterozygous G-to-A substitution in the second nucleotide of codon 445 in *OPA1*, resulting in an Arg-to-His amino acid substitution (p.R445H). He had no apparent family history of either optic atrophy or hearing impairment. At that time, he was also found to have a slight bilateral hearing impairment. The patient

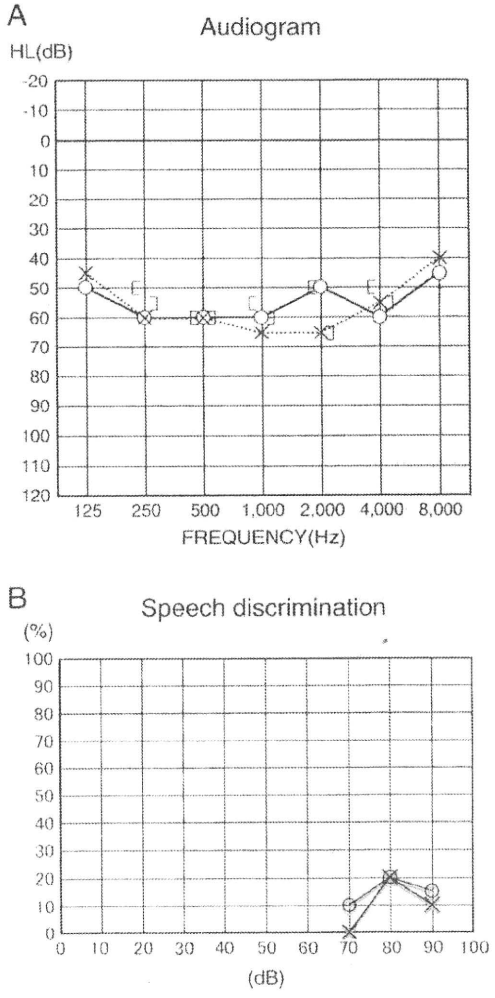

Fig. 1. Pure-tone (A) and speech (B) audiograms of a patient with an *OPA1* mutation. O = right air conduction hearing level; X = left air conduction hearing level; [= right bone conduction hearing level;] = left bone conduction hearing level.

developed progressive hearing impairment, and had particular difficulty understanding speech. He came to our department for a hearing evaluation at age 28. Although he did not initially complain of balance disorders, he stopped riding a bicycle at age 17 years because of difficulty controlling balance and also started to feel unsteady walking at that time. He thought the unsteadiness resulted from his visual dysfunction.

4. Results

4.1. Auditory function test results

Direct otoscopic observation revealed normal findings in both ears. A bilateral sensorineural hearing loss of approximately 60 dB was shown by pure-tone audiometry (Fig. 1A). The maximum speech discrimination scores were 20% in both ears (Fig. 1B), which were significantly worse than expected based on the results of pure-tone audiometry. Although no differences were observed between left and right ears, the patient reported better hearing discrimination in the right ear (Fig. 1). ABRs were absent bilaterally even at 100 dB nHL (Fig. 2A), but high-amplitude DPOAEs were present at all frequencies tested in both ears (Fig. 2B).

4.2. Vestibular function test results

No spontaneous, positioning, or pressure-induced nystagmus was found by electronystagmography. Neither 20 °C nor ice-water caloric stimulation of the labyrinth elicited nystagmus or dizziness in either ear (Fig. 3A). Short-tone burst-evoked VEMP analysis revealed a biphasic VEMP waveform in the right ear; however, the latency of n23, which is the second wave of VEMP, was delayed. No VEMPs were evoked in the left ear (Fig. 3B).

4.3. Neuroimaging studies

There were no abnormal findings by HRCT. In particular, no inner ear malformation or internal auditory canal stenosis was observed (Fig. 4A, D). By MRI, both the cochlear nerves and vestibular nerves were detected from brainstem to the inner ear in both ears in axial FIESTA slices (Fig. 4B, E). However, the diameter of the right cochlear nerve was 0.82 mm whereas that of the left cochlear nerve was 0.69 mm, and the diameter of the right facial nerve was 1.06 mm whereas that of the left facial nerve was 1.02 mm in oblique sagittal reconstructions through the IAC (Fig. 4C, F). Thus, the cochlear nerves on both sides are considered hypoplasia according to reported criteria [11].

4.4. OPA1 predicted structure

The distance between Cα of R445 of OPA1 and the GTP binding pocket is 18 Å (Fig. 5). The electric field around R445 is negatively charged due to its proximity to D450, D442, and E444. Under physiological conditions, positively charged R445 is structurally stable, and thus the mutation p.R445H reduces the electrostatic stability and indirectly distorts the structure of the GTPase catalytic

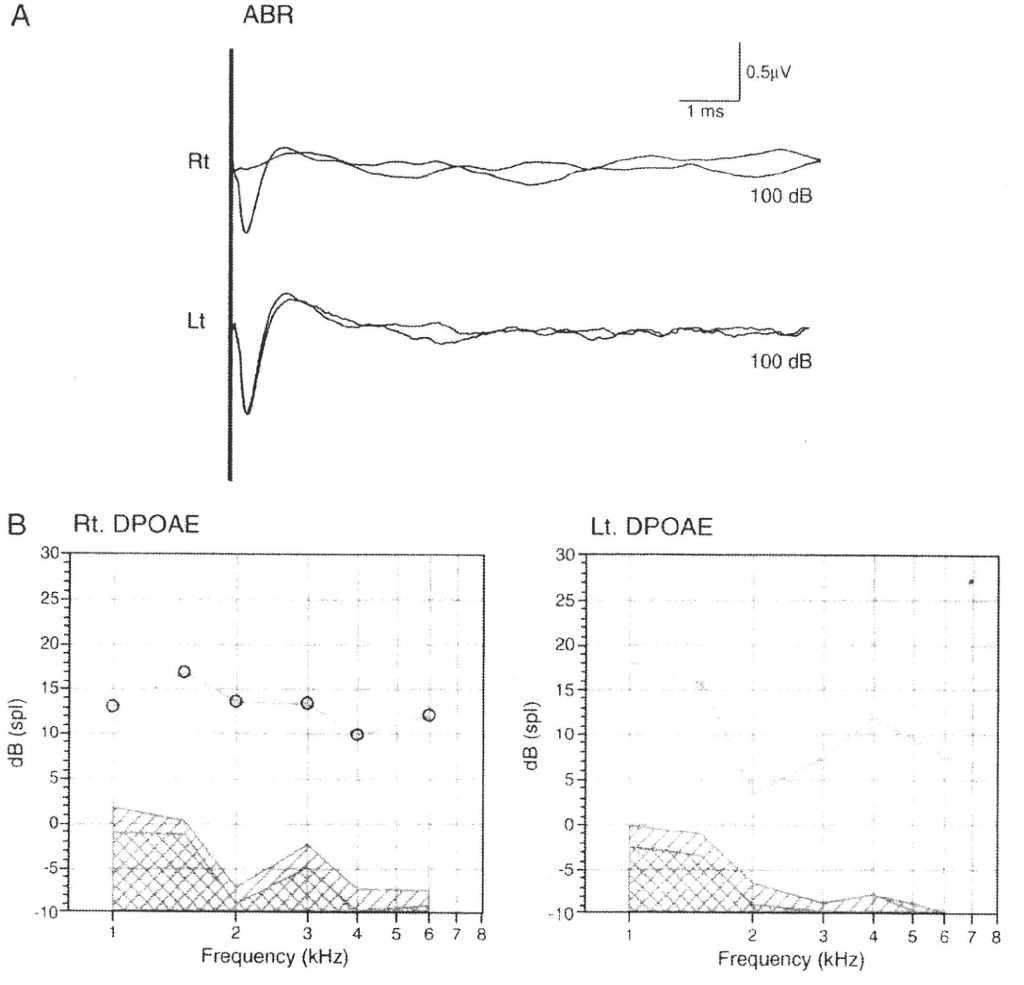

Fig. 2. (A) ABR tests revealed no ABR waveforms in this patient. (B) DPOAE recordings were normal for this patient. Residual noise levels are shown by the shaded area.

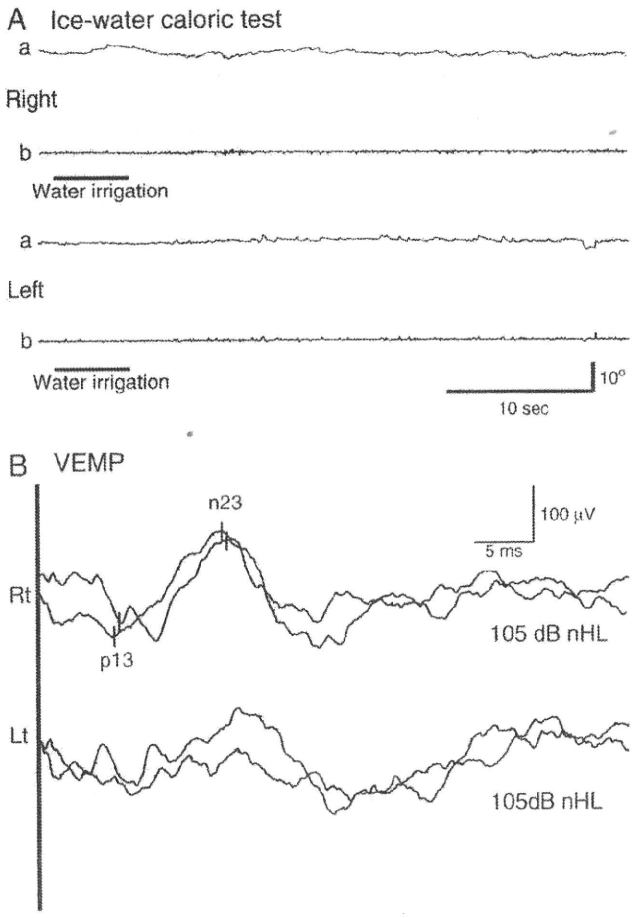

Fig. 3. (A) Horizontal record of electronystagmograph on ice-water caloric test. Time constants: a, 3.0 s; b, 0.03 s. No nystagmus were elicited in both side of ears. (B) Air-conducted VEMPs. Electromyographic responses of the right (Rt) and left (Lt) SCM to right ear stimulation. A biphasic VEMP waveform was revealed in the right ear; however, a latency of n23 was delayed. In contrast, no VEMPs were evoked in the left ear.

domain. In addition, salt bridges between R445 and D450 in the α3-helix and strong electrostatic interactions between R445 and D442/E444 are observed. The α3-helix is a key structure that constructs the common wire frame of the G-protein core fold [7,9]. Thus, the p.R445H mutation indirectly distorts the catalytic structure of the GTPase reaction center and decreases GTPase activity.

5. Discussion

Several reports have described hearing impairments associated with an *OPA1* mutation [4,12–16]. As with the case we present here, these hearing impairments were reported to result from auditory neuropathy. Common features in these patients include moderate hearing threshold elevation and a severe speech discrimination disability. No vestibular symptoms or function test results have yet been reported. To our knowledge, this is the first report of a detailed vestibular analysis in a patient with an *OPA1* mutation. Moreover, inner ear neuroimaging studies, including HRCT or 3-D MRI, have not yet been reported in patients with *OPA1* mutations. This report provides the first evidence of cochlear nerve atrophy in the IAC in a patient with an *OPA1* mutation.

OPA1 encodes a dynamin-related GTPase that is located in the mitochondrial intermembrane space and plays a key role in controlling the balance of mitochondrial fusion and fission [17]. Furthermore, release of cytochrome c from mitochondria and caspase-dependent activation of the apoptosis cascade have been observed in the down-regulation model of expression by RNA interference in HeLa cells [17]. The *OPA1* p.R445H mutation is reportedly associated with various neurological disturbances, including ataxia, peripheral neuropathy, ptosis, and cognitive impairment [18]. In cases involving the heterozygous p.R445H mutation, ADOAs associated with deafness have been reported [4], and these sensorineural hearing losses show audiological features compatible with auditory neuropathy. In normal rats, expression of OPA1 protein is seen in the inner hair cells, outer hair cells, and spiral ganglia in the cochlea, and in the vestibular hair cells and ganglia [6]. OPA1 protein expression has also been observed in membranous or submembranous compartments of vestibular ganglion cells and at the level of the calyx synapse, which typically envelopes type 1 hair cells in the vestibular epithelium [6]. Bilateral vestibular dysfunction in our present patient is probably caused by dysfunction of these parts of the vestibular organs.

An abnormality in the OPA1 protein may cause mitochondrial dysfunction, leading to insufficient energy production. Homozygous mutant mice are not viable and show impaired development as early E8.5. [19]. This study also reported that heterozygous mutants show a reduction in OPA1 protein level (about 50% compared with wild-type littermates) due to rapid degradation of the mutant polypeptide [19]. Skin fibroblasts obtained from patients carrying the heterozygous *OPA1* p.R445H mutation show hyperfragmentation of the mitochondrial network, decreased mitochondrial membrane potential, and an ATP synthesis defect [4]. Our three-dimensional structure study suggests that the p.R445H mutation reduces the electrostatic interactions and therefore the stability of the protein and indirectly distorts the structure of the GTPase catalytic center, thereby decreasing GTPase activity. According to these findings, we suggest that the OPA1 p.R445H mutation leads to severely insufficient energy production by decreasing GTPase activity in the mitochondria. This deficiency could, in turn, affect critical energy-dependent functions such as axoplasmic transport in both cochlear and vestibular nerve fibers as well as optic nerve fibers.

This patient had almost normal VEMP results in the right ear but no response in the left ear. Although the mechanisms underlying these different responses are unclear, asymmetrical hearing impairments have been reported in patients with the *OPA1* p.R445H mutation [12,13]. There was no response to caloric stimulation in either ear. The VEMP consists of myogenic potentials obtained as a response to tone-burst stimuli and is used to test the saccule and inferior vestibular nerve of the vestibular system. The caloric test, on the other hand, is used to evaluate the function of the lateral semicircular canals and the superior vestibular nerve [20]. In the right ear, there was no response in the caloric test but fare VEMPs. *OPA1* is expressed in sensory epithelia in both the saccule and the lateral semicircular canal [6]. Atrophy of the superior vestibular nerve was not detected by MRI scan. The mechanisms underlying different responses for the caloric test and VEMPs in the right ear are uncertain. In the present case, the patient reported slightly better hearing in the ear that also had good VEMP responses (the right ear). It is well established that ADOA is a progressive atrophy disease. If the main mechanism for nerve atrophy in ADOA is the same in both the eye and the inner ear, we speculate that nerve atrophy in the inner ear may develop gradually from the superior vestibular nerve to the inferior vestibular nerve in patients with the *OPA1* mutation. It has been reported that VEMPs are less affected than horizontal semicircular canal function during caloric testing in bilateral vestibulopathy [21]. We found only two reports with results of both caloric testing and VEMP analysis in auditory neuropathy patients with causes other than an *OPA1* mutation [20,22], and these revealed normal caloric responses and abnormal VEMPs in all patients ($n=4$) with auditory neuropathy. We revealed a different profile in a patient with auditory neuropathy due to an *OPA1* mutation. We speculate that the vestibule is also an organ that is sensitive to the mitochondrial dysfunction associated with the *OPA1* mutation.

In conclusion, we have presented a case of vestibular dysfunction accompanied with auditory neuropathy in a patient with an *OPA1*

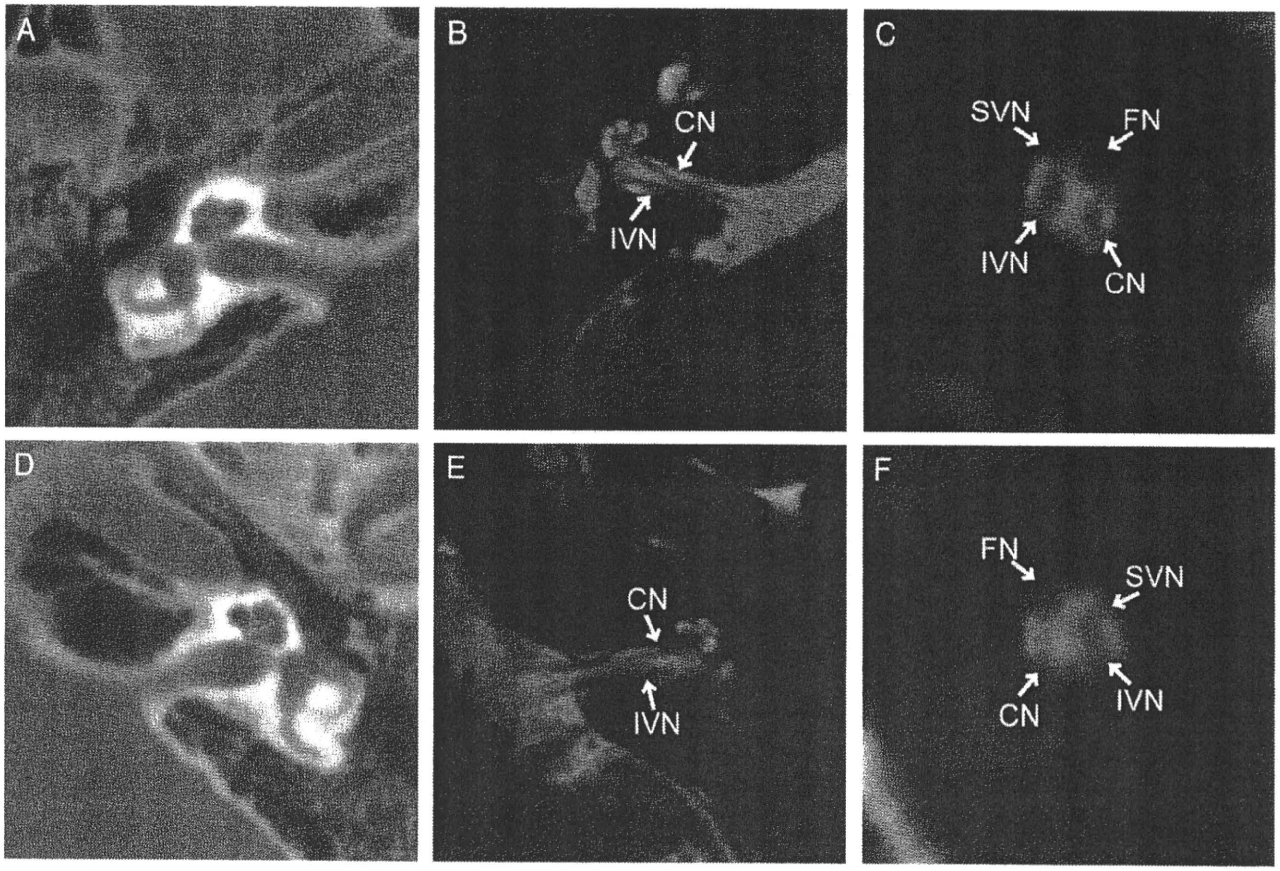

Fig. 4. Images showing the HRCT (A, D), axial MRI (FIESTA: B, E), and oblique sagittal reconstructions (C, F). The facial nerve (FN), cochlear nerve (CN), superior vestibular nerve (SVN), and inferior vestibular nerve (IVN) can be recognized in both sides of the internal auditory canal. However, the cochlear nerves in both ears were narrower than the vestibular nerves in axial FIESTA slices. Moreover, the cochlear nerves on both sides were smaller than the adjacent facial nerves in oblique sagittal reconstructions.

mutation. In a standard evaluation, this patient's balance disorder could easily have been overlooked because he attributed it to his visual dysfunction. Based on this case, we suggest that vestibular evaluation should be performed in auditory neuropathy patients carrying an *OPA1* mutation, even if the patients do not complain of balance dysfunction.

Acknowledgements

The authors give thanks to Ms. Reiko Yakushimaru and Ms. Akemi Hori for their excellent technical assistance in the audiometric and vestibular tests.

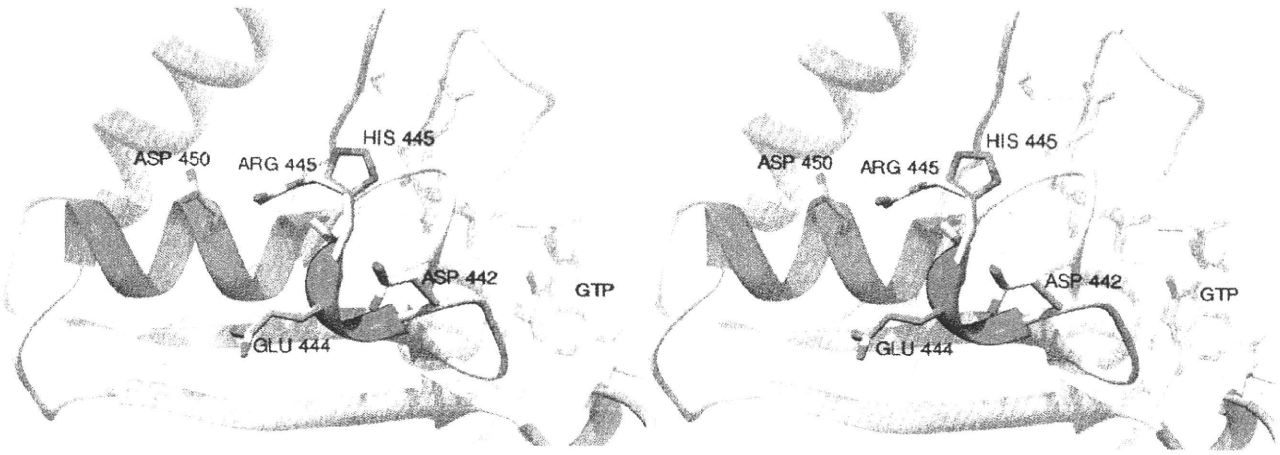

Fig. 5. Stereo view of the GTPase domain of predicted structure of human OPA1 with arginine at position 445 replaced by histidine. The electric field around R445 is negatively charged due to the proximity of D450, D442, and E444. Positively charged R445, under a physiological environment, is structurally stabilized, and thus the mutation p.R445H reduces the electrostatic stability and indirectly distorts the GTPase catalytic structure. Image produced using the UCSF Chimera package supported by NIH P41 RR-01081.

References

[1] Johnston RL, Seller MJ, Behnam JT, Burdon MA, Spalton DJ. Dominant optic atrophy. Refining the clinical diagnostic criteria in light of genetic linkage studies. Ophthalmology 1999;106:123–8.

[2] Eliott D, Traboulsi EI, Maumenee IH. Visual prognosis in autosomal dominant optic atrophy (Kjer type). Am J Ophthalmol 1993;115:360–7.

[3] Delettre C, Griffoin JM, Kaplan J, Dollfus H, Lorenz B, Faivre L, et al. Mutation spectrum and splicing variants in the *OPA1* gene. Hum Genet 2001;109:584–91.

[4] Amati-Bonneau P, Guichet A, Olichon A, Chevrollier A, Viala F, Miot S, et al. OPA1 R445H mutation in optic atrophy associated with sensorineural deafness. Ann Neurol 2005;58:958–63.

[5] Starr A, Sininger YS, Pratt H. The varieties of auditory neuropathy. J Basic Clin Physiol Pharmacol 2000;11:215–30.

[6] Bette S, Zimmermann U, Wissinger B, Knipper M. *OPA1*, the disease gene for optic atrophy type Kjer, is expressed in the inner ear. Histochem Cell Biol 2007;128: 421–30.

[7] Kaneko H, Kuriki T, Shimada J, Handa S, Takata H, Yanase M, et al. Modeling study of the neopullulanase–maltoheptaose complex. Res Commun Biochem Cell Mol Biol 1998;2:37–54.

[8] Holm L, Park J. DaliLite workbench for protein structure comparison. Bioinformatics 2000;16:566–7.

[9] Pettersen EF, Goddard TD, Huang CC, Couch GS, Greenblatt DM, Meng EC, et al. UCSF Chimera — a visualization system for exploratory research and analysis. J Comput Chem 2004;25:1605–12.

[10] Shimizu S, Mori N, Kishi M, Sugata H, Tsuda A, Kubota N. A novel mutation in the *OPA1* gene in a Japanese patient with optic atrophy. Am J Ophthalmol 2003;135: 256–7.

[11] Glastonbury CM, Davidson HC, Harnsberger HR, Butler J, Kertesz TR, Shelton C. Imaging findings of cochlear nerve deficiency. Am J Neuroradiol 2002;23:635–43.

[12] Payne M, Yang Z, Katz BJ, Warner JE, Weight CJ, Zhao Y, et al. Dominant optic atrophy, sensorineural hearing loss, ptosis, and ophthalmoplegia: a syndrome caused by a missense mutation in OPA1. Am J Ophthalmol 2004;138:749–55.

[13] Li C, Kosmorsky G, Zhang K, Katz BJ, Ge J, Traboulsi EI. Optic atrophy and sensorineural hearing loss in a family caused by an R445H OPA1 mutation. Am J Med Genet A 2005;138A:208–11.

[14] Chen S, Zhang Y, Wang Y, Li W, Huang S, Chu X, et al. A novel OPA1 mutation responsible for autosomal dominant optic atrophy with high frequency hearing loss in a Chinese family. Am J Ophthalmol 2007;143:186–8.

[15] Huang T, Santarelli R, Starr A. Mutation of *OPA1* gene causes deafness by affecting function of auditory nerve terminals. Brain Res 2009;1300:97–104.

[16] Hogewind BF, Pennings RJ, Hol FA, Kunst HP, Hoefsloot EH, Cruysberg JR, et al. Autosomal dominant optic neuropathy and senseorineural hearing loss associated with a novel mutation of WFS1. Mol Vis 2010;16:26–35.

[17] Cipolat S, Martins de Brito O, Dal Zilio B, Scorrano L. OPA1 requires mitofusin 1 to promote mitochondrial fusion. Proc Natl Acad Sci USA 2004;101:15927–32.

[18] Amati-Bonneau P, Valentino ML, Reynier P, Gallardo ME, Bornstein B, Boissiere A, et al. OPA1 mutations induce mitochondrial DNA instability and optic atrophy 'plus' phenotypes. Brain 2008;131:338–51.

[19] Alavi MV, Bette S, Schimpf S, Schuettauf F, Schraermeyer U, Wehrl HF, et al. A splice site mutation in the murine *OPA1* gene features pathology of autosomal dominant optic atrophy. Brain 2007;130:1029–42.

[20] Sheykholeslami K, Schmerber S, Habiby Kermany M, Kaga K. Sacculo-collic pathway dysfunction accompanying auditory neuropathy. Acta Otolaryngol 2005;125:786–91.

[21] Zingler VC, Weintz E, Jahn K, Botzel K, Wagner J, Huppert D, et al. Saccular function less affected than canal function in bilateral vestibulopathy. J Neurol 2008;255:1332–6.

[22] Akdogan O, Selcuk A, Ozcan I, Dere H. Vestibular nerve functions in children with auditory neuropathy. Int J Pediatr Otorhinolaryngol 2008;72:415–9.

Pediatr Radiol (2010) 40:1509–1516
DOI 10.1007/s00247-010-1609-7

ORIGINAL ARTICLE

CT and MR imaging for pediatric cochlear implantation: emphasis on the relationship between the cochlear nerve canal and the cochlear nerve

Mikiko Miyasaka · Shunsuke Nosaka · Noriko Morimoto · Hidenobu Taiji · Hidekazu Masaki

Received: 10 October 2009 / Revised: 16 January 2010 / Accepted: 15 February 2010 / Published online: 23 March 2010

Abstract
Background Cochlear implantation has become an accepted treatment for deafness. As the frequency of cochlear implantation has increased, requests for images have also increased in the work-up for candidates. An absent cochlear nerve (CN) is a contraindication to cochlear implantation. Therefore, MRI is performed to evaluate the CN in patients with sensorineural hearing loss. Recently, some authors have reported the relationship between cochlear nerve canal (CNC) stenosis and CN hypoplasia.
Objective To review the relationship between CNC and CN.
Materials and methods During a period of 78 months, 21 children (42 ears) with unilateral or bilateral sensorineural hearing loss underwent both HRCT and MRI of the cochlear nerve. We retrospectively reviewed two factors: the evaluation of inner ear malformations and the relationship between CNC stenosis and CN hypoplasia.
Results Inner ear malformations were recognized in ten ears. The mean CNC diameter was approximately 2 mm (ranging from 0.6 to 2.7 mm). CN hypoplasia was seen in eight of the 42 ears; all eight were associated with CNC stenosis (≤1.5 mm). Of the 34 ears with normal CN, 32 had CNC >1.5 mm in diameter and the remaining two ears, with incomplete partition type I, had CNC stenosis.
Conclusion Children with CNC stenosis had a high incidence of CN hypoplasia. CNC stenosis (≤1.5 mm) suggests CN hypoplasia. On the other hand, CN hypoplasia was not seen in children with CNC diameter >1.5 mm. Therefore, we conclude that children with CNC stenosis or malformations on HRCT should receive MR imaging of the CN.

Keywords Cochlear implantation · Cochlear nerve · Cochlear nerve canal · Children

M. Miyasaka (✉) · S. Nosaka · H. Masaki
Department of Radiology,
National Center for Child Health and Development,
2-10-1 Okura, Setagaya-ku,
Tokyo 157-8535, Japan
e-mail: Miyasaka-m@ncchd.go.jp

N. Morimoto · H. Taiji
Department of Otolaryngology,
National Center for Child Health and Development,
Tokyo, Japan

Introduction

Hearing loss is one of the most common birth defects, affecting 3–4 of every 1,000 newborns [1]. A variety of pathologic conditions cause hearing loss in children [2]. With the advent of universal newborn screening, deafness can be diagnosed earlier in life [3].

Cochlear implantation has become an accepted treatment for deafness. As the frequency of cochlear implantation has increased, requests for imaging have also increased in the work-up of cochlear implant candidates. Radiologists must be familiar with imaging findings that contraindicate implantation (cochlear aplasia and cochlear nerve aplasia) [4]. High-resolution CT (HRCT) of the temporal bone has been used to evaluate mastoid air cell aeration, facial nerve position, and inner ear malformations. On the other hand, MRI is better to visualize the cochlear nerve and intracranial structure directly . Therefore, high-resolution MRI has been used to detect CN aplasia or hypoplasia in children with sensorineural hearing loss (SNHL) [1, 3–6]. Recently, some authors have reported a relationship between cochlear nerve canal stenosis and CN hypoplasia [7–9]. Those findings have important implications for clinicians who evaluate children with SNHL. CNC stenosis might be a key

finding to select children with SNHL who should undergo further evaluation with MRI.

The purposes of this study were to evaluate a variety of pathological conditions for children with SNHL and to review the relationship between CNC and CN.

Materials and methods

This study was reviewed and approved by the ethics committee of our hospital.

During a period of 78 months, 21 children (42 ears) with unilateral or bilateral SNHL underwent both high-resolution CT of the temporal bone and MRI of the cochlear nerve (Table 1). These 21 children included eight boys and 13 girls, with a mean age of 7 years (ranging from 1 to 13 years) at the time of the MRI. Of these, 11 children had unilateral and ten children had bilateral SNHL (31 ears with SNHL and 11 without). Cochlear implantation was performed in three children who had bilateral SNHL and a normal CN.

The protocol of HRCT of the temporal bone was performed with a multidetector-row CT scanner (8-detector,

Fig. 1 Measurement of CNC on axial image of temporal HRCT. The CNC is the bony canal from the fundus of the IAC to the base of the modiolus. The diameter of the CNC width (*line*) was measured along the inner margin of its bony walls at its middle portion on an axial image of the base of the modiolus

Table 1 Summary of CT and MRI findings in children with SNHL

Case no.	Age (years) /sex	Side of SNHL	Inner ear malformations		CNC diameter (mm)		CN on MRI	
			Right	Left	Right	Left	Right	Left
1	8/F	Right	Michel deformity	No	–	2	Absent	Normal
2	2/F	Bilateral	Cochlear aplasia	Cochlear aplasia	–	–	Absent	Absent
3	10/F	Left	IP-I	IP-I	1.2	1.0	Normal	Normal
4	11/M	Bilateral	Large vestibular aqueduct syndrome	Large vestibular aqueduct syndrome	2.0	2.0	Normal	Normal
5	13/F	Right	Duplication of IAC	No	0.68	2	Absent	Normal
6	6/F	Bilateral	Large vestibular aqueduct syndrome	Large vestibular aqueduct syndrome	2.1	2	Normal	Normal
7	5/F	Bilateral	No	No	2	1.9	Normal	Normal
8	1/M	Right	No	No	1.5	2	Absent	Normal
9	2/F	Bilateral	No	No	2.2	2.1	Normal	Normal
10	6/F	Right	No	No	2.2	2.1	Normal	Normal
11	8/M	Bilateral	No	No	2.4	2.4	Normal	Normal
12	10/M	Left	No	No	2.4	2.5	Normal	Normal
13	5/F	Bilateral	No	No	2.1	2.1	Normal	Normal
14	3/F	Bilateral	No	No	2.5	2.2	Normal	Normal
15	5/M	Left	No	No	1.9	–	Normal	Hypoplasia
16	7/F	Right	No	No	0.59	1.8	Hypoplasia	Normal
17	7/M	Right	No	No	2.2	1.8	Normal	Normal
18	13/M	Right	No	No	2.5	2.7	Normal	Normal
19	13/F	Bilateral	No	No	2.4	2.6	Normal	Normal
20	7/F	Right	No	No	1.5	2.4	Hypoplasia	Normal
21	3/M	Bilateral	No	No	2.1	2.2	Normal	Normal

SNHL sensorineural hearing loss, *CNC* cochlear nerve canal, *CN* cochlear nerve, *M* male, *F* female, *No* no abnormality, –not evaluated, *IP-I* Incomplete partition type I

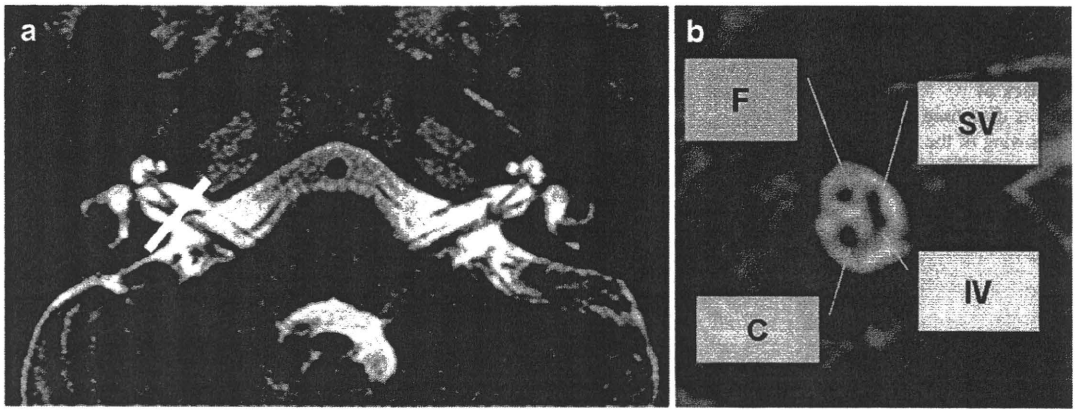

Fig. 2 Axial and oblique sagittal image of normal IAC on DRIVE. **a** Axial image of the cerebellopontine region and IAC shows the normal anatomy. Line illustrates the plane prescribed for oblique plane sagittal images obtained perpendicular to the nerves of the IAC. **b** Oblique sagittal image obtained at the fundus of the IAC, oriented with anterior to the left and the cerebellum to the right. Four nerves were recognized. *F:* Facial nerve, *C:* Cochlear nerve, *SV:* Superior vestibular nerve, *IV:* Inferior vestibular nerve

LightSpeed Ultra, GE, Milwaukee, WI, USA). Images were acquired in the direct axial planes using a 0.625-mm slice thickness, a field of view (FOV) of 96 mm, 140 kV, 150 mA, 1.25 pitch, and a bone algorithm. CT was performed with the minimal radiation dose, according to the ALARA (as low as reasonably achievable) concept. The radiation dose ranged from 35.55 mGy to 44.44 mGy for CT dose index volume ($CTDI_{vol}$). We are now using low kV and mA to lower the $CTDI_{vol}$. Coronal multi-planar reconstruction images were obtained, as well. The CNC is a bony canal extending from the fundus of the inner auditory canal (IAC) to the base of the modiolus. The diameter of the CNC was measured along the inner margin of its bony walls at its middle portion on an axial image of the base of the modiolus (Fig. 1).

All MR images were obtained using a 1.5-T or 1.0-T magnet (Intera 1.5T and 1.0T; Philips, The Netherlands). The children were studied in the supine position with a head coil. The MRI scan sequences included a 3-D T2-weighted fast spin-echo sequence (using DRIVE: driven equilibrium) in axial and oblique sagittal planes of the IAC with a 0.7-mm slice thickness and an FOV of 130 mm. Oblique sagittal images were obtained perpendicular to the course of the nerves through the IAC (Fig. 2). The scan time was approximately 30 min. In oblique sagittal images of the lateral aspect of the IAC, four nerves were recognized (facial, superior vestibular, inferior vestibular and cochlear).

We retrospectively reviewed the following factors: (1) the evaluation of the inner ear malformations on HRCT, (2) the CNC measurements on HRCT, (3) the presence of CN hypoplasia or aplasia on MRI, (4) the relationship between CNC stenosis and CN hypoplasia or aplasia. The cochleovestibular malformations were listed according to the new classification system for inner ear malformations (Table 2), published in 2002 by Sennaroglu and Saatci [10]. As Kim et al. [11] reported, the CN is larger than either the superior or inferior vestibular nerve in 90% of normal ears and is of similar size or larger than the facial nerve in 65%. Therefore, we designated the CN as hypoplastic when it appeared smaller than the facial nerve and as aplastic when it could not be identified on oblique sagittal images.

Results

Evaluation of inner ear malformations on HRCT

Of the 42 ears, cochlear malformations were recognized in ten ears (six children). The details of the inner ear malformations were as follows: Michel deformity in one ear, cochlear aplasia in two ears, incomplete partition type I (IP-I) in two ears (Fig. 3), large vestibular aqueduct syndrome in four ears, and duplication of IAC in one ear (Fig. 4) [12–15].

CNC measurements on HRCT

Of the 42 ears, four ears without a CNC could be evaluated. These four ears had Michel deformity (one ear), cochlear

Table 2 A new classification for inner ear malformations [10]

-Michel deformity
-Cochlear aplasia
-Common cavity deformity
-Cochlear hypoplasia
-Incomplete partition type I (IP-I)
-Cochlear hypoplasia
-Incomplete partition type II (IP-II) = Mondini deformity

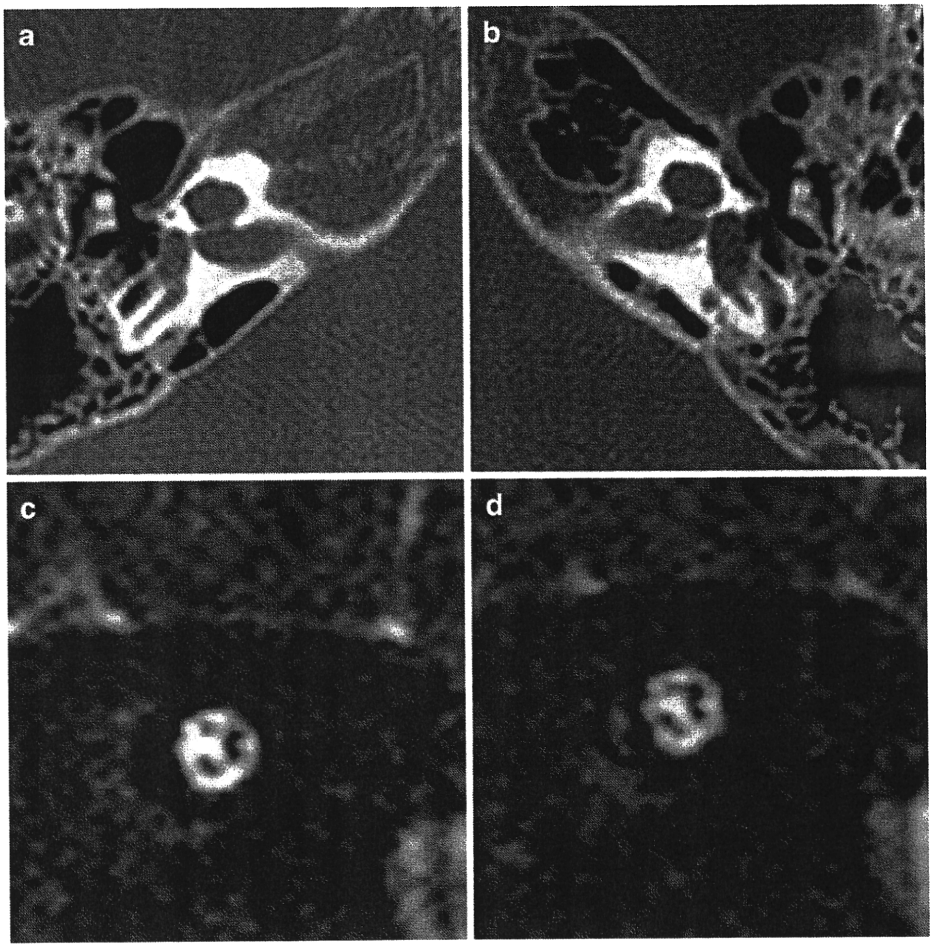

Fig. 3 IP-I in a 10-year-old girl with left SNHL (case 3). **a, b** Axial images show cystic cochlea and the lack of modiolus, which is diagnosed as IP-I. The narrowing of the CNC is also seen. **c, d** Oblique sagittal DRIVE images show normal CN, bilaterally

aplasia (two ears) and a closed CNC without cochlear dysplasia (one ear).

The CNC was measurable in the remaining 38 ears. The CNC diameters ranged from 0.6 mm to 2.7 mm in 27 ears with SNHL and from 1.2 mm to 2.7 mm in 11 ears without SNHL. The mean CNC diameter was 2 mm in each ear, with or without SNHL.

Presence of CN hypoplasia or aplasia on MRI

The CN of all ears could be evaluated on MRI. CN hypoplasia and aplasia were seen in three and five ears, respectively. These corresponded to the affected side. The remaining 23 ears with SNHL and 11 ears without SNHL had a normal CN.

The relationship between CNC stenosis and CN hypoplasia/aplasia (Table 3)

All eight ears with CN hypoplasia or aplasia were associated with CNC stenosis (CNC diameter ≤1.5 mm; mean, 1.1 mm). The remaining 34 ears had a normal CN. Of these, 32 ears had normal CN and CNC diameters >1.5 mm (mean, 2.2 mm). Despite CNC stenosis (<1.5 mm), normal CN was seen in two ears with IP-I. A CNC with CN hypoplasia or aplasia was smaller than those with a normal CN.

Of the eight ears with CN hypoplasia or aplasia, four had inner ear malformations, as follows: one with Michel deformity, two with cochlear aplasia, and one with duplication of the IAC. The remaining four ears with CN hypoplasia or aplasia failed to show inner ear malformation (Fig. 5). On the other hand, four ears with large vestibular aqueduct syndrome and two ears with IP-I did not have CN hypoplasia, and three ears had CN hypoplasia without inner ear malformations. CN aplasia without inner ear malformation was seen in one ear.

Discussion

A variety of pathologic conditions cause SNHL in infants and children [2]. Recent studies suggest that cochlear nerve dysfunction accounts for up to 10% of newly diagnosed

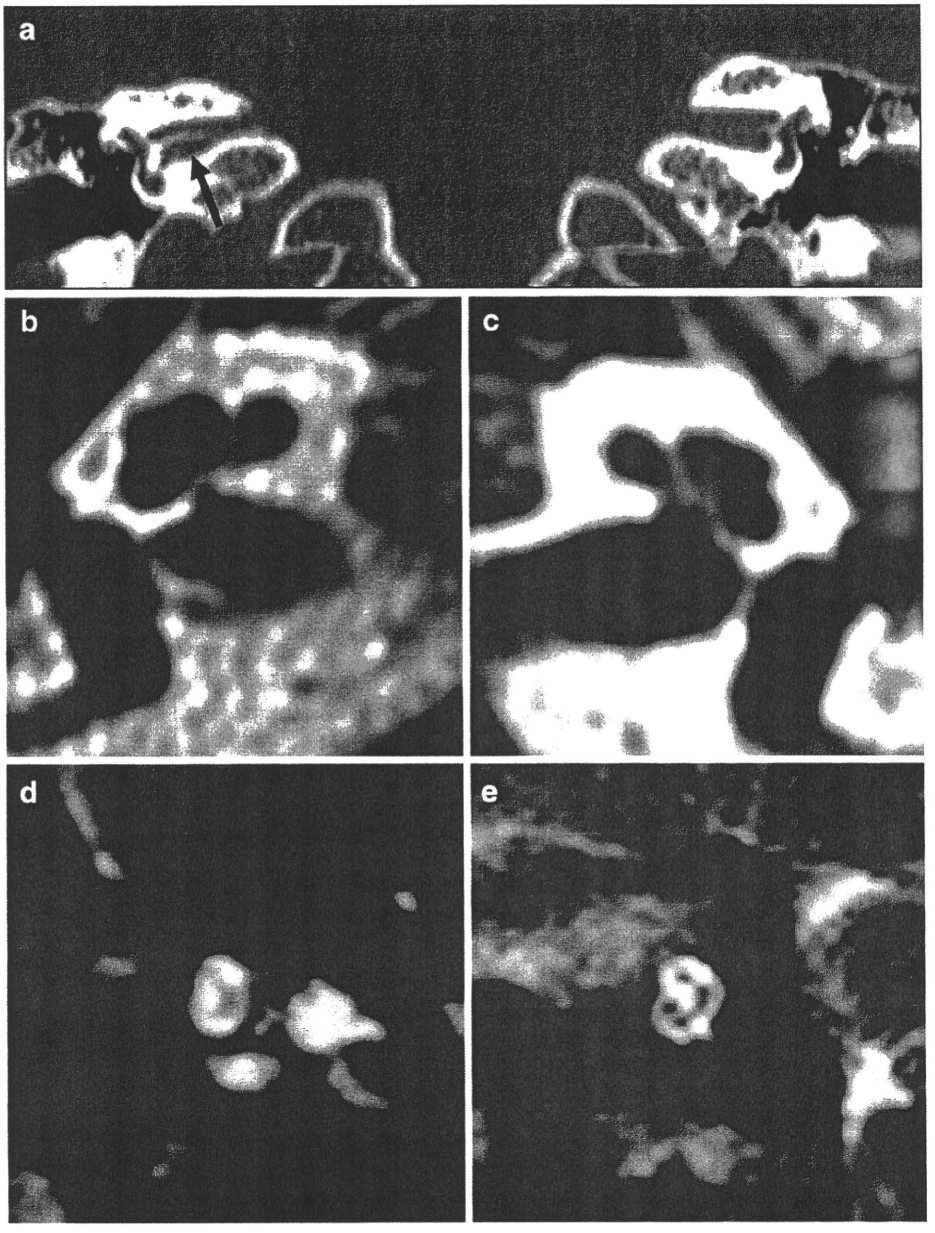

Fig. 4 Duplication of IAC in a 13-year-old girl with right SNHL (case 5). **a** Coronal reconstructed image shows narrowing of right IAC and a bony septum in the right IAC (*arrow*). **b, c** On axial images, narrowing of right CNC (0.68 mm) is recognized compared with the left CNC (2 mm). **d** On oblique sagittal DRIVE image, the right CN is unclear, while the left (**e**) is normal. Diagnosis of the duplication of the IAC associated with CN aplasia was made by referring to previous reports [12–15]

cases of SNHL in children [1]. Imaging plays an important part in the work-up of cochlear implant candidates [4]. Traditionally, HRCT has been the imaging modality of choice in the initial work-up of these children [16]. On the other hand, MR has advantages in detecting soft-tissue abnormalities, especially those of the facial-vestibulocochlear nerves [17], which are best recognized on 3-D FRFSE (3-D fast recovery fast spin-echo) or 3-D CISS (3-D constructive interference in steady state) images [5]. Therefore, MRI is accepted as the method of choice to evaluate abnormalities in candidates for cochlear implants. Opinion varies regarding the advantages of HRCT versus MRI as an initial imaging modality for a cochlear implant candidate [4, 17].

The incidence of children with SNHL who show inner ear malformations on HRCT ranges from 20% to 30% [16, 18]. In the present study, inner ear malformations were present in six of 21 cases (29%). The children had a variety of inner ear malformations. These results were similar to those of the previous reports [16, 18].

Pathologically, both congenital deficiency and acquired degeneration of the CN have been seen in children with SNHL [6]. Jackler et al. [19] and Shelton et al. [20] suggested that the presence of a narrow IAC on HRCT was indicative of CN aplasia. The vestibulocochlear nerve starts to develop at approximately 3 weeks of gestation. At 9 weeks, the IAC is formed by the build-up of cartilage

Table 3 The relationship between CNC stenosis and CN hypoplasia/aplasia (n=42 ears)

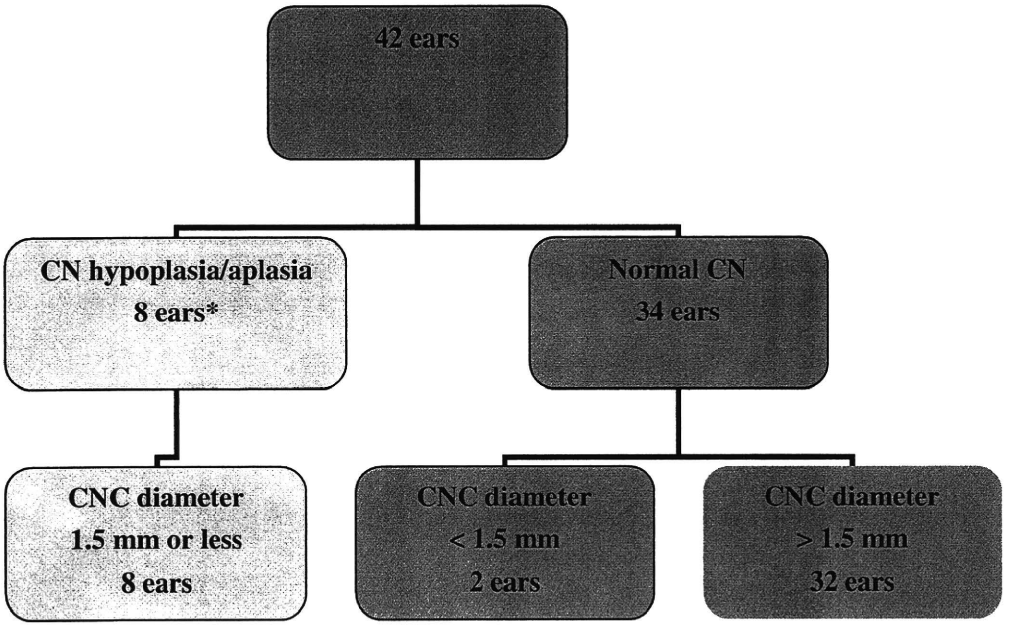

*CN hypoplasia/aplasia	8 ears
Associated with inner ear malformations	4 ears
Michel deformity	1 ear
Cochlear aplasia	2 ears
Duplication of IAC	1 ear
No association with inner ear malformations	4 ears

with development of the nerve. Therefore, the IAC cannot form in the absence of the nerve [5, 6, 9]. In a report by Casselman et al. [5], CN hypoplasia or aplasia was detected with or without labyrinth anomalies. Additionally, some authors reported cases of CN aplasia with normal IAC dimensions [21, 22]. The causes of acquired CN deficiency are complex. CN deficiency can result from degeneration of the nerve fibers in the IAC after cochlear injury (e.g., vascular, traumatic, compressive, or inflammatory injury). Therefore, the findings of a normal-size IAC with CN deficiency suggest an acquired cause of SNHL [6]. In the present study, CN hypoplasia or its aplasia was diagnosed in eight ears (19%) on MRI. Of these, four ears had inner ear malformations and four did not. Histories of infection or trauma were unclear in the four ears with malformations. However, it is possible that infections or trauma are secondary to acquired CN hypoplasia.

Fatterpekar et al. [8] reported that hypoplasia of the CNC was a possible cause of congenital SNHL. Since then, some authors have reported a relationship between CNC stenosis and CN hypoplasia [7–9, 21]. The cause of a small CNC is unclear. Embryologically, the soft tissue of the inner ear is formed after the bony labyrinth. Some authors have suggested that abnormal development of the membranous labyrinth has a trophic effect on the CN. In addition to the development of the IAC, the CNC might require stimulation by its contents for normal development. Accordingly, CNC stenosis might be secondary to CN hypoplasia [7]. Stjernholm et al. [23] determined that if the CNC was less than 1.4 mm in diameter, then the possibility of CN abnormality should be considered. In a report by Komatsubara et al. [9], patients with a narrow CNC on CT studies were diagnosed as having CN hypoplasia on MRI with 88.9% sensitivity and 88.9% specificity. Those authors stated that in ears in which CNC was <1.5 mm on CT, CN hypoplasia could be seen on MRI. In a report by Kono [7], a CNC diameter <1.7 mm suggested CN hypoplasia, even if no cochlear abnormality could be found on CT. In the present study, all eight ears with CN hypoplasia had a small CNC (≤1.5 mm). This result is similar to that of Komatsubara et al. [9]. Only two ears of IP-I with a small CNC had no CN hypoplasia and the reasons for the small CNC in these cases

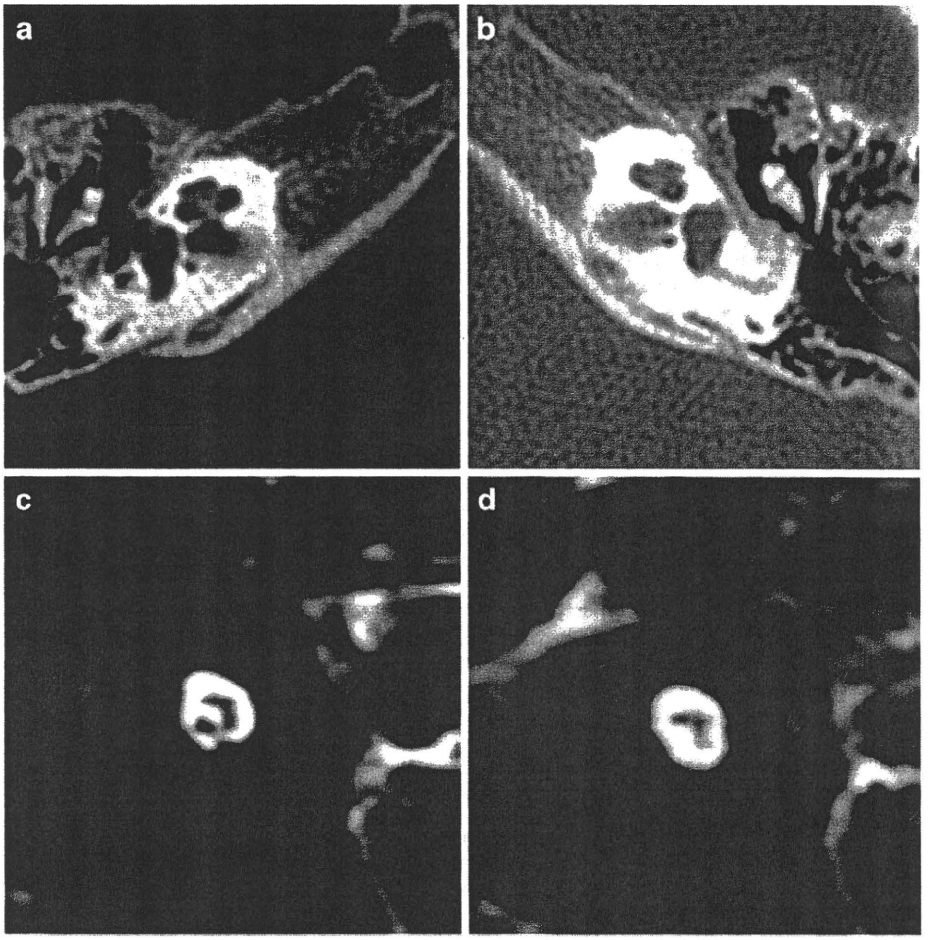

Fig. 5 Narrowing of the CNC without inner ear malformations in a 5-year-old boy with left SNHL (case 15). **a** Axial HRCT image shows no significant abnormality of the cochlea on the right. The diameter of CNC was 1.9 mm. **b** Axial image of the left side shows no significant abnormality of cochlea, but severe CNC stenosis is revealed. **c** The right CN appears to be normal compared with the facial nerve on oblique sagittal DRIVE image. In contrast, the left cochlear nerve (**d**) is small

are unknown. On the other hand, CN appeared to be normal in cases with a CNC diameter >1.5 mm in both affected and unaffected ears. Therefore, noting the presence of CNC stenosis helped to confirm the diagnosis of CN hypoplasia or aplasia [21]. However, our study was limited to a small series in one institution and was a retrospective study. Larger prospective studies are necessary to examine these issues.

Maxwell et al. [24] reported that they used MRI as the initial investigation method and reserved CT for special situations. MRI can be used to evaluate the CN complex directly regardless of the IAC size or whether the CNC is small or large [16]. We understand their recommendation, but we believe there are several drawbacks to using MRI as the initial modality. MRI cannot show the course of the facial canal or allow for a detailed evaluation of inner ear malformations. Moreover, it is a longer procedure, and most children younger than 6–8 years need sedation, possibly general anesthesia, to undergo MRI successfully [2, 23]. On the other hand, the disadvantage of CT is the radiation exposure. However, CT can be easily and quickly utilized in almost all situations. Moreover, CNC stenosis (CNC diameter ≤1.5 mm) helped to confirm the likely diagnosis of CN hypoplasia or its aplasia [9]. If CNC stenosis or cochlear malformation is revealed on HRCT, the additional MRI in these selected children might show CN aplasia or hypoplasia. MRI can confirm the status of CN, whether there is aplasia or hypoplasia, and help predict the degree of improvement in hearing performance after implantation. Therefore, the finding of CNC stenosis might be used to select children with SNHL who should undergo further evaluation with MRI. We believe that CT administered with the ALARA concept is useful and acceptable for children with SNHL. On the basis of these findings, we recommend CT for the initial screening of candidates for cochlear implantation.

Conclusion

CT and MR imaging are both useful in children with SNHL. There was a high incidence of CN hypoplasia or aplasia associated with cochlear anomalies and CNC stenosis. CNC stenosis with a diameter of 1.5 mm or less suggests CN hypoplasia or aplasia. On the other hand, CN hypoplasia was not seen in children with CNC stenosis with a diameter

greater than 1.5 mm. Therefore, we conclude that children with CNC stenosis (≤1.5 mm) or with severe inner ear malformations on HRCT require MR imaging of the CN.

References

1. Adunka OF, Roush PA, Teagle HF et al (2006) Internal auditory canal morphology in children with cochlear nerve deficiency. Otol Neurotol 27:793–801
2. Lowe LH, Vezina LG (1997) Sensorineural hearing loss in children. Radiographics 17:1079–1093
3. Russo EE, Manolidis S, Morriss MC (2006) Cochlear nerve size evaluation in children with sensorineural hearing loss by high-resolution magnetic resonance imaging. Am J Otolaryngol 27: 166–172
4. Witte RJ, Lane JI, Driscoll CL et al (2003) Pediatric and adult cochlear implantation. Radiographics 23:1185–1200
5. Casselman JW, Offeciers FE, Govaerts PJ et al (1997) Aplasia and hypoplasia of the vestibulocochlear nerve: diagnosis with MR imaging. Radiology 202:773–781
6. Glastonbury CM, Davidson HC, Harnsverger HR et al (2002) Imaging findings cochlear nerve deficiency. AJNR 23:635–643
7. Kono T (2008) Computed tomographic features of the bony canal of the cochlear nerve in pediatric patients with unilateral sensorineural hearing loss. Radiat Med 26:115–119
8. Fatterpekar GM, Mukherji SK, Alley J et al (2000) Hypoplasia of the bony canal for the cochlear nerve in patients with congenital sensorineural hearing loss: initial observations. Radiology 215:243–246
9. Komatsubara S, Haruta A, Nagano Y et al (2007) Evaluation of cochlear nerve imaging in severe congenital sensorineural hearing loss. ORL J Otorhinolaryngol Relat Spec 69:198–202
10. Sennaroglu L, Saatci I (2002) A new classification for cochleovestibular malformations. Laryngoscope 112:2230–2241
11. Kim HS, Kim DI, Chung IH et al (1998) Topographical relationship of the facial and vestibulocochlear nerves in the subarachnoid space and internal auditory canal. AJNR 19:1155–1161
12. Ferreira T, Shayestehfar B, Lufkin R (2003) Narrow, duplicated internal auditory canal. Neuroradiology 45:308–310
13. Demir OI, Cakmakck H, Erdag TK et al (2005) Narrow duplicated internal auditory canal: radiological findings and review of the literature. Pediatr Radiol 35:1220–1223
14. Weon YC, Kim JH, Choi SK et al (2007) Bilateral duplication of the internal auditory canal. Pediatr Radiol 37:1047–1049
15. Bail HW, Yu H, Kim KS et al (2008) A narrow internal auditory canal with duplication in a patient with congenital sensorineural hearing loss. Korean J Radiol 9:S22–S25
16. McClay JE, Booth TN, Parry DA et al (2008) Evaluation of pediatric sensorineural hearing loss with magnetic resonance imaging. Arch Otolaryngol Head Neck Surg 134:945–952
17. Trimble K, Blaser S, James AL et al (2007) Computed tomography and/or magnetic resonance imaging before pediatric cochlear implantation? Developing an investigative strategy. Otol Neurotol 28:317–324
18. Shim HJ, Shin JR, Chung JW et al (2006) Inner ear anomalies in cochlear implants: importance of radiologic measurements in the classification. Otol Neurotol 27:831–837
19. Jackler RK, Luxford WM, House WF (1987) Congenital malformations of the inner ear: a classification based on embryogenesis. Laryngoscope 97:2–14
20. Shelton C, Luxford WM, Tonokawa LL et al (1989) The narrow internal auditory canal in children: a contraindication to cochlear implants. Otolaryngol Head Neck Surg 100:227–231
21. Adunka OF, Jewells V, Buchman CA et al (2007) Value of computed tomography in the evaluation of children with cochlear nerve deficiency. Otol Neurotol 28:597–604
22. Sennaroglu L, Saatci I, Aralasmak A et al (2002) Magnetic resonance imaging versus computed tomography in pre-operative evaluation of cochlear implant candidates with congenital hearing loss. J Laryngol Otol 116:804–810
23. Stjernholm C, Muren C (2002) Dimension of the cochlear nerve: a radioanatomic investigation. Acta Otolaryngol 122:43–48
24. Maxwell AP, Mason SM, O'Donoghue GM (1999) Cochlear nerve aplasia: its importance in cochlear implantation. Am J Otol 20:335–337

Audiology Japan 53, 76～83, 2010

Auditory neuropathy spectrum disorder の乳幼児例における ASSR 閾値

泰地秀信[1]，守本倫子[1]，松永達雄[2]

[1]国立成育医療センター耳鼻咽喉科

[2]国立病院機構東京医療センター耳鼻咽喉科・臨床研究センター

要旨：Auditory neuropathy は2008年の国際会議から ANSD と呼称されており，今回はその定義に従って診断された ANSD の乳幼児９例について検討した。後に ABR が正常化していくようなみかけ上の難聴例（auditory immaturity）は除外した。経過をみていくうちに DPOAE が消失した５例は ANSD とみなした。ASSR の閾値にはかなり大きなばらつきがあり，ANSD の病態が多彩であることが推定された。良聴耳の ASSR 閾値と COR 閾値を比較したところ，500～4000Hz では有意な相関が認められた。ANSD の場合も補聴器装用効果を ASSR でとらえることができ，推測された利得は平均でみて COR との差は 10dB 以下であった。３例は ASSR の３分法平均の閾値が 70dBHL 未満で，その場合 COR の平均閾値も 88dBHL 以下と他症例より良好であったが，これらはすべて基礎疾患を伴っていた。ASSR および COR 閾値が 100dBHL 以上の重度難聴の例のうち２例に *OTOF* 遺伝子変異が認められた。ASSR は ANSD で行動聴力検査が不確実な場合に聴力および補聴器装用効果を評価する方法になりうるものと考えられた。

ーキーワードー

乳幼児聴力検査，聴性脳幹反応，歪成分耳音響放射

はじめに

Auditory neuropathy は耳音響放射（OAE）が正常で聴性脳幹反応（ABR）が無反応あるいは異常となる病態で，聴力に比し語音聴取力が低いことが特徴とされているが，その臨床像はさまざまであり，2008年に公表されたガイドラインでは auditory neuropathy spectrum disorder（以下 ANSD と略）と呼称されることになった[1]。ANSD については補聴器の効果あるいは人工内耳手術の適応などまだ意見の一致がみられていない点が多いため，今回は ANSD の乳幼児例について ASSR 検査を行い，他の所見と対比検討したので報告する。

対象と方法

平成18年４月～平成21年３月に国立成育医療センター耳鼻咽喉科を受診した新生児・乳幼児で，DPOAE の反応が両側正常かつ ABR 閾値が両側 80 dBnHL 以上で ANSD として扱った症例のうち，当院で療育・聴覚管理を行うことになった９例に ASSR 検査を行った。NICU 児では中枢系の未成熟のために ABR の閾値上昇・波形分離不良がみられることがあり，ANSD と診断されても ABR が発達とともに正常化することがある。Berg らの報告[2]では NICU 児の24％に ANSD がみられているが，我々の検討[3]では NICU 児で ABR 閾値上昇がみられた場合，19％は１歳時に 20dB 以上閾値が改善している。今回はそのような例は除外するために，１

歳を過ぎてもABR閾値が改善しないもの，あるいは初回のABR検査が1歳以上で行われたものを対象とした。またOAEが初期に正常でその後に消失した場合はANSDに含めるとされているので[1]，経過をみていくうちにDPOAEが消失した例も対象に含めた。ANSDの診断にはMRIにて蝸牛神経欠損を除外する必要があるものとされているが[1]，MRIまたはCTにて蝸牛神経欠損と考えられた例は除外した。なお，今回の検討例では9例中7例にMRIまたはCTを行っている。

ABRは日本光電MEB-2204（Neuropack）により測定した。鎮静下に検査を行い，刺激にはクリック音を用いて10dBステップで閾値を求めた。DPOAEはOAE analyzer ER-32（Grason-Stadler社製）またはHLO292（Otodynamics社製）を用いて記録した。DPOAEの刺激音圧はL1＝65dB SPL，L2＝55dB SPLで，また測定条件はOAE analyzerおよびHLO292ともにデフォルトの設定通りとした。両耳ともOAE analyzerでpassと判定されたもの，あるいはHLO292で測定9周波数（1～6kHz）のうち8周波数以上がノイズレベルより5dB以上高いものをDPOAE正常とした。対象者の概略を表1に示すが，月齢は平均7.7ヶ月（±8.1 SD，SDは標準偏差），性別は男児5例，女児4例であった。基礎疾患として，9例のうち6例に難聴のリスクファクターが認められた。ABR閾値は7例がクリック105 dBnHLで両側無反応で，1例が両側90dBnHL，1例が右80dBnHL，左100dBnHLであった。

ASSR検査にはGrason-Stadler社製Audera を使用した。ASSRの刺激音は250，500，1k，2k，4kHzのAM/FM複合音を用い（変調周波数はそれぞれ67，74，81，88，95Hz），鎮静下に検査を行った。ASSR検査は年齢が7ヵ月～4歳のときに測定した。ABRおよびASSR検査ともに鎮静はトリクロホスナトリウム内服で行い，十分な鎮静が得られない場合は抱水クロラール坐薬を追加した。ASSRは推定聴力レベルではなく，実際の閾値（反応の得られた最小の刺激音圧）について検討したが，250Hzでは110dB HL，500Hzでは120dB HL，1～4kHzでは125dB HLで反応がなければ無反応とした。またASSRは10dBステップで閾値を求めたが，1～4kHzについては120dB HLで反応がない場合，125 dB HLでも測定を行った。

さらに条件詮索反応聴力検査（COR）による聴覚評価も行い，比較検討した。COR検査の値は症例8を除いては，2～3歳での測定値を集計した。ASSRの方がCORよりやや行った時期が早い例が多いが，CORについては検査の精度を高めるため2～3歳での値をとっている。症例8は年齢が1歳6ヵ月より前のため，CORは1歳時に測定した値である。CORは250Hzでは95dB HL，500Hzでは100dB HL，1～4kHzでは110dB HLで反応がなければ無反応とした。

また，全例に補聴器装用を行っているが，7例には補聴器を装用してのASSR検査を行った。片耳ずつ補聴器を装用し，ASSRに外付けしたスピーカ（FE207E）から刺激音を提示し，ASSR測定を行った。なおスピーカは1m離れたところにおき，音圧校正を行ってから測定を行った（自由音場でのセットとして設定）。補聴器装用時のASSRについても閾値につき検討したが，250Hzでは70dB，500Hzでは80dB，1kHzでは85dB，2，4kHzでは90dBで反応がなければ無反応とした。補聴器両耳装用時のCOR閾値も全例で測定しているので，補聴器装用でのASSR検査を行った7例につき比較検討を行った。

結　果

DPOAEは症例9（初診が平成21年）を除き反復して測定を行っているが，5例は経過をみているうちにDPOAEの反応が消失した（表1）。DPOAEの反応が消失した5例のうち基礎疾患があるものは4例で，DPOAEが保たれている4例のうち基礎疾患があるものは2例であった。

図1に9例18耳についてのASSR閾値の分布を示す。大きなばらつきがあることがわかった。無反応の場合は閾値として最大の測定音圧に＋5dBした値をとり，3分法平均（500，1k，2k Hz）のASSR閾値を求めたが（表1，図1），うち3例6耳は3分法平均の閾値が70dBHL未満であった。これは症例1，5，7であり，すべて基礎疾患を伴っている例であった。うち2例はDPOAEが経過で消失していた。ASSR閾値（左右別）およびCOR閾値の平均を比較したものを図2に示す。CORについて

表1 症例の概略
DPの経過で+はDPが保存されていることを示す。
ASSR閾値は3分法平均の値を示す。

症例	受診時月齢	性	基礎疾患	ABR	DPの経過	ASSR右閾値	ASSR左閾値
1	6	F	TTTSドナー，超低出生体重児	無反応	消失	63(dB)	57(dB)
2	6	M	なし	無反応	消失	100	107
3	5	M	超低出生体重児，高ビリルビン血症	無反応	消失	113	107
4	0	M	なし	無反応	+	103	113
5	5	F	超低出生体重児，脊髄空洞症	両側90dB	消失	67	53
6	5	F	超低出生体重児，脳性麻痺	無反応	消失	128	127
7	10	M	West症候群，脳性麻痺	無反応	+	67	67
8	5	M	高ビリルビン血症（核黄疸）	右80dB，左100dB	+	110	110
9	28	F	なし	無反応	+	97	107

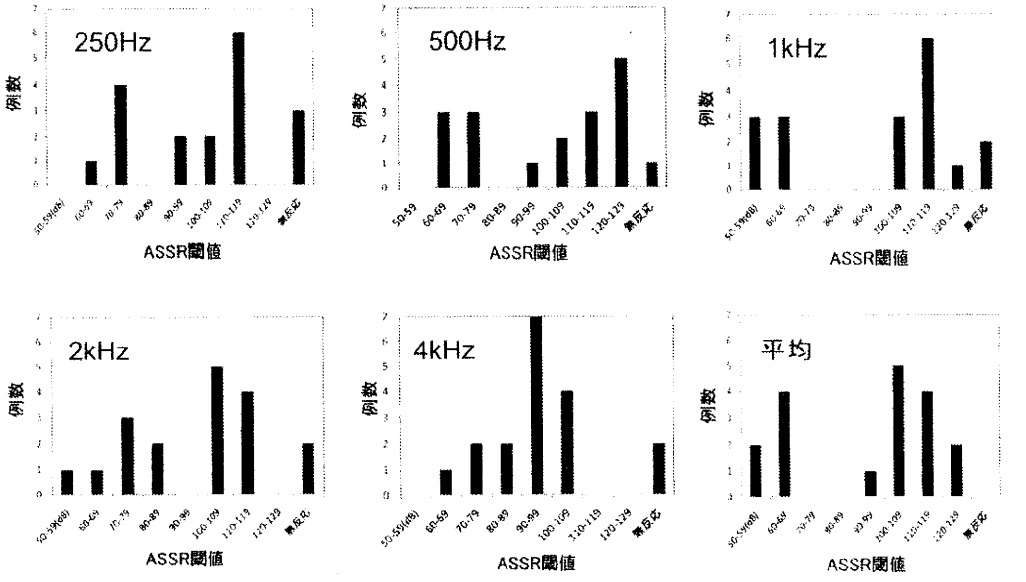

図1 周波数別にみた裸耳でのASSR閾値の分布（9例18耳）
ばらつきが大きく，3例6耳の閾値は平均が70dBHL未満である

も，無反応と判定した場合は最大の測定音圧に+5dBした値を集計した。1～4kHzについてはCORの方が測定の最大音圧が小さいにもかかわらず，ASSRより閾値の平均値が大きかった。CORの3分法平均（500，1k，2k Hz）の閾値は9例の平均が96dBHLであるが，ASSR閾値が良好（3分法平均が70dBHL未満）の3例についてはCORの平均閾値も80，70，88dB HLと他症例より良好であった。ASSRとCORの閾値の相関をみるために，ASSRの左右別の閾値のうち良好な方の値とCOR閾値を周波数別に比較してみた。図3に全測定周波数の結果をまとめた散布図を示す。良聴耳のASSR閾値とCOR閾値の相関係数は，250Hzが0.616，500Hzが0.836，1kHzが0.922，2kHzが0.769，4kHzが0.755で，500Hz，1kHzについては有意水準1%，2kHz，4kHzについては有意水準5%で有意な相関が認められた。

ASSR閾値は7例14耳で補聴器装用時について自由音場で測定を行ったので，結果を図4に示す。裸耳のときと同様にばらつきはかなり大きかった。補聴器装用時のASSR閾値の3分法平均が50dBHL未満のものが4耳みられたが，これは症例1，5の結

果（2例4耳）であり，裸耳のASSR閾値が良好なものは補聴器装用時のASSR閾値も良好であった。なお症例7は補聴器装用時の3分法平均ASSR閾値が左右とも60dBHLであった。また図5に補聴器装用での左右別ASSR閾値およびCOR閾値の平均を比較したものを示すが，これでは差はほとんどなかった。ASSRおよびCORについて裸耳の閾値から補聴器装用時の閾値を差し引くことにより推定した補聴器の利得の各周波数での平均を図6に示す。なお，補聴器装用時の閾値がスケールアウトの場合は利得を0として計算した。500Hz～4kHzについては，平均で15dB以上の利得がASSRおよびCORともにみられた。CORの方がASSRより推定される利得が良好な傾向があったが，その差は10dB以下であった。

考　察

ANSDはOAEが正常でABRが無反応あるいは異常となる病態で，当初はauditory neuropathyある

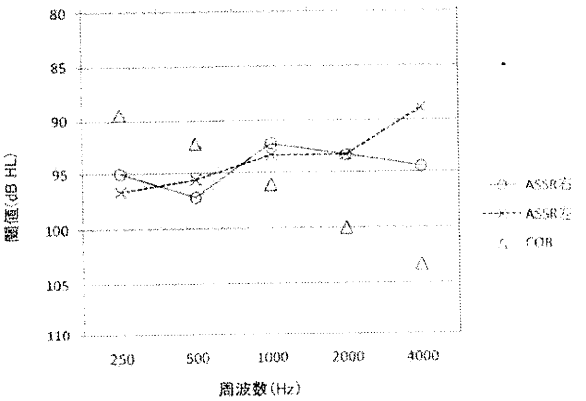

図2　裸耳でのASSR閾値およびCOR閾値の平均
CORの平均値は高音漸減型となった。

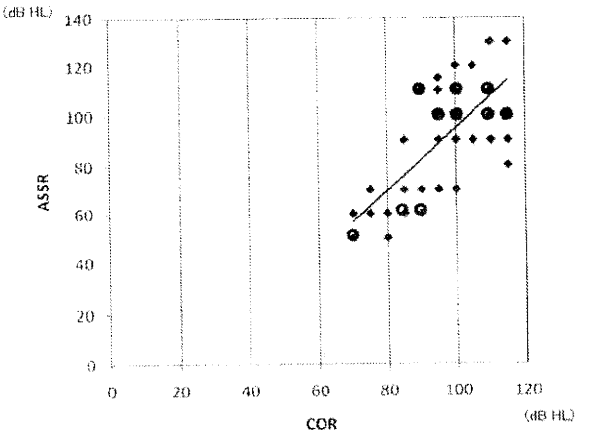

図3　ASSR閾値とCOR閾値の比較
全データの分布を示す。図中に回帰直線を記した。
複数のデータが重なる点は●を重ねて示した。

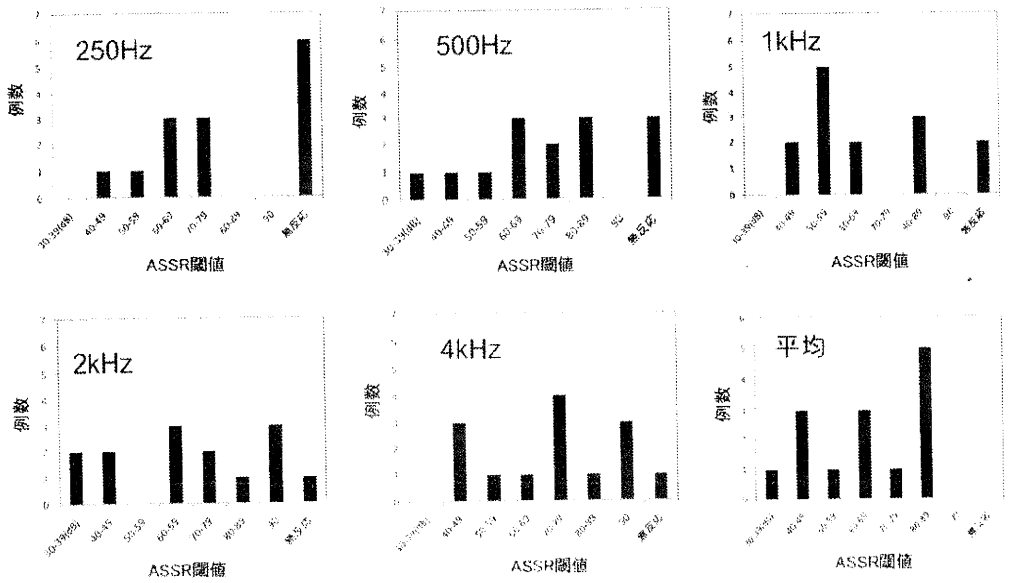

図4　周波数別にみた補聴耳でのASSR閾値の分布（7例14耳）
裸耳と同様に症例ごとのばらつきが大きい。

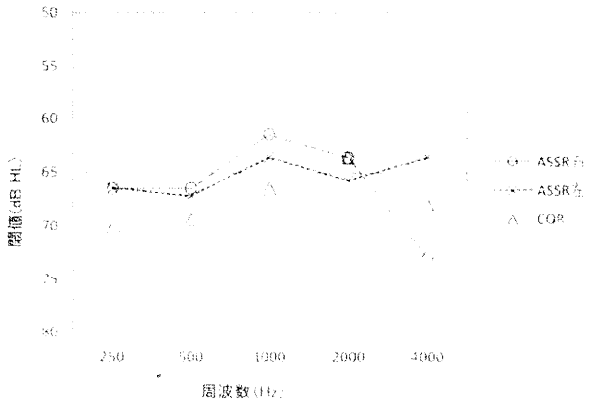

図5 補聴耳でのASSR閾値およびCOR閾値の平均
平均ではASSRとCORの閾値にあまり差はみられない

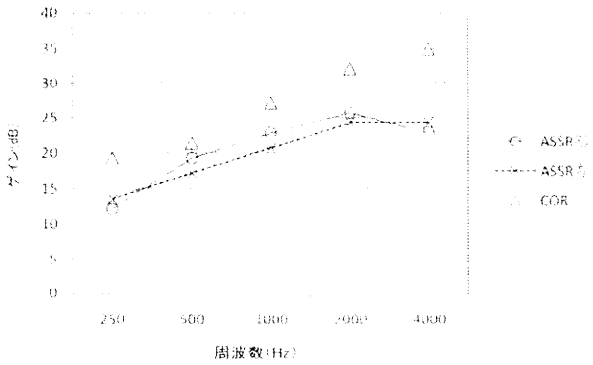

図6 ASSR閾値およびCOR閾値から推定された補聴器の利得の平均
推定される利得はCORの方がASSRよりやや大きい

いはauditory nerve diseaseと呼ばれていたが[1]，2008年の国際新生児聴覚スクリーニング会議でANSDと呼称されることになった[2]．ANSDでは聴力障害の程度はさまざまであり，言語発達も正常のこともあれば全く語音が認識できず言語発達がみられないこともある[1]．聴力障害の程度に比べ語音聴取力が悪く，言語発達の良好な例でも雑音下では語音聴取が困難という特徴がある．なおABRが無反応であっても聴力がないということではなく[3]，ANSDには後にABRが正常化してくる例がある．そのようなABRでのみかけ上の難聴（髄鞘化不全などによる）はauditory immaturityとして真のANSDとは区別されるべきものとされており，今回はそのような例を除外するために対象は1歳時でABR無反応あるいは閾値が両側80dBnHLのものとした．

ANSDは外有毛細胞の機能が正常で聴覚の求心性神経経路の障害があるものと考えられている[4]．診断にはMRIにて蝸牛神経の欠損あるいは低形成を除外する必要がある[5]が，今回の9例のうち4例にはMRI（3-D CISS撮像）を行い蝸牛神経は正常であることを確認している．3例には側頭骨CTを行っており，いずれも内耳道・蝸牛神経管に異常はみられていないので蝸牛神経欠損は否定的である．残る2例（症例1，9）については画像検査を行っていないが，両側ともに蝸牛神経欠損である可能性は低いものと思われる．またOAEが初期に正常で後に消失した場合はANSDに含めるとされているので[1]，今回は経過をみていくうちにDPOAEが消失した5例もANSDとみなした．DPOAEが保存されているとした4例についても，症例8は年齢が1歳6ヵ月以下であり，2歳を過ぎて保たれているのは3例である．ANSDの概念は1996年より報告されているのに，新生児聴覚スクリーニングが開始（本邦ではモデル事業が2001年から）されてからANSDの報告が増えているのは，中途でOAEが消失する例が多いためかもしれない．

ANSDではABRやASSRで聴覚閾値を測定することは困難とされている[1]．今回はANSD例にAuderaを用いASSR測定を行ったが，図1に示すように閾値にはかなり大きなばらつきがあり，ASSRからもANSDの病態が多彩であることが推定された．80-Hz ASSRの起源もABRと同様に脳幹と考えられているが，その機序は異なるものと推定されており[6]，そのためABR無反応例でASSR閾値がさまざまとなったものと思われる．ASSRはABRと異なり活動電位の同期を必要としないので[6]，ANSDでASSRが検出されることは十分あり得る[7]．左右別のASSR閾値およびCOR閾値の平均を比較したところ（図2），CORはASSRに比べて低音域では閾値が低く，高音域では閾値が高い傾向があった．250Hz，500HzでASSRの閾値が比較的高いのは他の感音難聴例でも同じ[7]であり，ASSRは位相の同期性の有無を確率的に判定するので周期の長い低音域では検出しにくいためと考えられる．青柳は500Hz以下で80-Hz ASSRの閾値と聴力レベルとの相関が低くなる理由として聴覚フィルタを想定している[7]．高音域でCORとASSRが異なる理由

は不明であるが，これはASSR閾値が実際より低いのではなく，CORの精度が児の発達遅滞（9例のうち4例に重複障害）により低くなり閾値が高くなったためとも考えられる。なお，以前に我々がANSD以外のABR無反応例についてASSR閾値を調べた結果では[8]，1kHzが最も閾値が低かった。

ASSR閾値がかなり良好な症例（両耳とも3分法平均の閾値が70dBHL以下）が3例あり，そのような例ではCORの平均閾値も88dBHL以下（それ以外の例はすべて96dBHL以上）と良好であり，ASSRとCORの閾値には一致した傾向がみられた。良聴耳のASSR閾値とCOR閾値を比較したところ（図3），ばらつきはあるものの正の相関があり，周波数別に相関をみると500Hz～4kHz（250Hz以外）では有意な相関が認められた。ASSR閾値が真の聴覚閾値を示すかどうかは今後さらに検討が必要であるが，行動聴力検査と高い相関があったということはANSDの聴力の指標になり得るものと考えられた。

ANSDに対する補聴器の装用効果がみられる例は限られているとされているが[1]，今回の検討例はすべて両耳に補聴器装用を行っている。聴能訓練を行い，2例（症例3，5）は年齢相応の言語発達が認められたが，3例（症例2，4，9）は合併疾患がないのに発語は全くみられていない。ANSDで後にOAEが消失する場合は補聴効果が期待できるとした報告[7]があるが，症例3，5は経過観察中にDPOAEが消失した。補聴器装用時のASSR閾値（表3）にはかなりのばらつきがあるが，裸耳のASSR閾値が良好な例（症例1，5，7）は補聴器装用時の閾値も良好（平均が左右とも60dBHL以下）であった。補聴器装用時のASSR閾値とCOR閾値の比較（図5）では，裸耳のときと違い低音域ではASSRの方がやや良好な傾向がみられたが，これは250Hz，500Hzでは音場検査でのASSRの最大音圧が小さく（それぞれ70，80dBHL）スケールアウトの値も小さくなったためと考えられる。補聴器装用効果については，図6に示すように平均でみてASSRでも十分にとらえられており，補聴器の評価としてのASSRの有用性が示唆された。図6でCOR閾値からみた2，4kHzでの補聴器の利得がかなり大きくなっているのは，この周波数帯での裸耳のCOR平均閾値が高いためである。なお，ANSDでは補聴器装用により静かなところでの語音の聞き取りは改善するが，雑音下での聞き取りは困難とされており[10]，今回示された補聴効果よりも言語獲得のための補聴器の有効性は低くなることが予想される。ANSDでの人工内耳の効果は他の重度感音難聴と変わらないので[7]，補聴器の効果が十分でないANSDでは人工内耳が検討されるべきであるが，前述したauditory immaturity（一過性のANSD）の可能性を考え手術適応の決定には行動聴力検査を含めた十分な聴力評価が必要である。

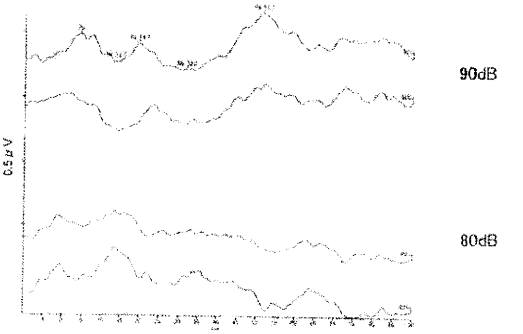

図7　ANSD例におけるCAEP検査の測定例
1000Hz，左耳での測定例で，90dBで明瞭に反応（MLR）が認められる。

なおANSDにおいてABR検査を行うときには極性を変えたクリック音（rarefaction, condensation）を用いることが推奨されているが[10]，今回はalternating clickで検査を行った。また，ANSDにおいて行動聴力検査の結果が不確かなときは皮質誘発反応（Cortical auditory evoked potentials：CAEPs）が有用であるとされており[1]，我々も3例にAuderaを用いてCAEPsの測定を行った。結果の例を図7に示すが，測定した3例はすべて発語のみられない例であったのにもかかわらずCAEPsは反応があり，本検査の意義は今後の課題である。ANSDでは*OTOF*，*PMP22*，*MPZ*，*NDRG1*などの遺伝子変異が報告されているが[11]，今回の症例では2例に*OTOF*遺伝子変異が認められた。*OTOF*遺伝子変異のみられた2例はASSRおよびCORの平均閾値がいずれも100dBHL以上の重度難聴であり，補聴器装用効果も少ないため1例は人工内耳手術を行った。

ま と め

1．Auditory neuropathyは2008年の国際会議からANSDと呼称されており，今回はその定義に従って診断されたANSDの9例について検討した。経過をみていくうちにDPOAEが消失した5例もANSDとみなした。

2．ASSRの閾値にはかなり大きなばらつきがあり，ANSDの病態が多彩であることが推定された。良聴耳のASSR閾値とCOR閾値を比較したところ，500Hz～4kHzでは有意な相関が認められた。

3．ANSDの場合も補聴器装用効果をASSRでとらえることができ，推測された利得は平均でみてCORとの差が10dB以下であった。

4．3例はASSRの3分法平均の閾値が70dBHL未満で，その場合CORの平均閾値も88dBHL以下と他症例より良好であった。これらはすべて基礎疾患を伴っている例であった。ASSRおよびCOR閾値が100dBHL以上の重度難聴の例のうち2例に*OTOF*遺伝子変異が認められた。

（本研究は厚生労働省　成育医療研究委託費（17公—3）「新生児・乳幼児難聴の診断および療育に関する研究（主任研究者：泰地秀信）」および平成21年度厚生労働科学研究　感覚器障害研究事業「日本人小児難聴におけるAuditory Neuropathyの診療指針の確立（主任研究者：松永達雄）」による研究成果である）

Auditory steady-state response thresholds in infants and young children with auditory neuropathy spectrum disorder

Hidenobu Taiji[1], Noriko Morimoto[1], Tatsuo Matsunaga[2]

[1]Department of Otolaryngology, National Center for Child Health and Development
[2]Department of Otolaryngology/Lab. of Auditory Disorders, National Institute of Sensory Organs, National Tokyo Medical Center

Auditory neuropathy, renamed by consensus at a recent international conference as auditory neuropathy spectrum disorder (ANSD), is a specific form of hearing loss defined by normal otoacoustic emissions, but severely abnormal or completely absent auditory brainstem responses. We investigated the distribution of auditory steady-state response (ASSR) thresholds in 9 infants and young children with ANSD. The large variability of ASSR thresholds indicated the heterogeneous nature of this disorder. Correlation values showed a significant positive relationship ($p<0.05$) between ASSR and conditioned orientation response audiometry (COR) thresholds at 500–4000Hz. To estimate the functional gains obtained from the use of hearing aids, we examined the dB difference between unaided and aided thresholds of ASSR and COR. The average functional gains estimated by the ASSR thresholds were up to 15 dB at 500–4000Hz, which were slightly lower than those estimated by the COR thresholds. ASSR testing is considered to be useful for hearing aid validation when behavioral test methods are inconclusive. ASSR may be useful for the estimation of residual auditory capacities and hearing aid benefits in infants and very young children with ANSD.

文　献

1）Roush P：Auditory neuropathy spectrum disorder：Evaluation and management. Hearing Journal **61**：36–41, 2008
2）Berg AL, Spitzer JB, Towers HM, et al：Newborn hearing screening in the NICU：Profile of failed auditory brainstem response/passed otoacoustic emission. Pediatrics **116**：933–938, 2005
3）泰地秀信：厚生労働科学研究"新生児・乳幼児難聴の診断および療育に関する研究"平成17–19年度総括・分担報告書。2008, pp1–380
4）Buchman C, Roush P, Teagle H, et al：Auditory neuropathy characteristics in children with cochlear nerve deficiency. Ear Hear **27**：399–408, 2006